IJAME
Int. J. of Applied Mechanics and Engineering, 2024, vol.29, No.1, pp.90-104
DOI: 10.59441/ijame/181556

THE DETRIMENTAL EFFECT OF THERMAL EXPOSURE AND THERMOPHORESIS ON MHD FLOW WITH COMBINED MASS AND HEAT TRANSMISSION EMPLOYING PERMEABILITY

Ashik Hussain Mirza
Mathematics, Debraj Roy College, INDIA

Bamdeb Dey*
Mathematics, Assam Don Bosco University, INDIA
E-mail: bamdeb.dey@dbuniversity.ac.in

Rita Choudhury
Mathematics, Gauhati University, INDIA

We look at the viscous free-convective transitional magnetohydrodynamic thermal and mass flow over a plate that is always perforated and standing upright through permeable media while thermal radiation, a thermal source, and a chemical reaction are all going on. There is additional consideration for the Soret effect. The plate receives a normal application of a transversely consistent magnetic field. The magnetic Reynolds number is considerably lower considering the axial applied magnetic field instead of the induced magnetic field. The models that control mass, heat, and fluid flow are turned into two-dimensional shapes, and the answers are found by running numerical simulations using the MATLAB algorithm bvp4c. In realistic circumstances, the outcomes have been illustrated graphically. Several fluid properties have been found to have an impact on velocity, temperature, and concentration profiles. There is noticeable increase in velocity along with the growth of the permeability parameter and Soret number. Other dimensionless parameters have a significant impact on the fluid velocity. Likewise, the temperature profile diminishes as the radiation parameter has increased. The concentration distribution falls as the heat source parameter expands. Also, the analysis is encompassed in tabular form for the shearing stress, Nusselt number, and Sherwood number. The combined knowledge of heat and mass moving through viscous flows can be used to make a wide range of mechanisms and processes. These include biological reactors, therapeutic delivery systems, methods of splitting, aerodynamic aircraft design, and modeling for sustainability. It also optimizes automotive radiators and engine efficiency, and it improves cooling systems.

Keywords: thermal radiation, chemical reaction, heat source, Soret effect, heat and mass transfer.

1. Introduction

The concurrent transmission of mass and heat is an extremely important system that has been thoroughly researched. In recognition of the broad spectrum of potential applications that viscous fluid flow issues with thermal radiation and the Soret effect are currently demonstrating interest in applications in engineering, physics, and technology process sectors. More distinctively, it has a wide utility in aerospace technology, temperature processes, and the construction of pertinent apparatus. Over the past few decades, there has been a lot of interest in chemical reactions as a collective heat and mass transmission flow problem due to their significant status in many chemical manufacturing techniques. A few examples of such models encompass haze creation and dispersal, damage to crops caused by thawing, food preparation, cooling facilities, temperature imitation, and moisture

* To whom correspondence should be addressed

circulation. Agricultural fields and forests made of plant-based trees are just two more examples.

Numerous researchers have talked about the importance of the conveyance of heat energy caused by the thermal variation and the distribution of heat caused by the degree of concentration disparity. R. D. Ene *et al.* [1] analyze the issue of heat and mass transport rationally in a viscous flow. They found that with the growth of the Prandtl number, the deceleration of fluid temperature is observed which reflects the release of more heat. As a result, the heat transfer rate increased. I. H. Qureshi *et al.* [2] have explored the numerical research of the transfer of warmth and energy in MHD nanofluid flow behaviour in a medium with porosity, and they came across that the appropriate temperature soared when radiation emerged from the frictional force and was transferred to the fluid's molecule constituents. Thermal and energy diffusion in MHD micropolar fluid movement over a stretchable plate, along with momentum and thermoslip parameters, have been studied by E. O. Fatunmbi and A. Adeniyan [3]. B. G. Agaiel *et al.* [4] analysed the heat and mass transport of MHD prior to an unsteady viscous oscillatory stream and came to the conclusion that the diffusion coefficient proportion also causes changes in temperature as well as velocity contour. G. P. Vanitha *et al.* [5] investigated the exchange of heat and mass in the micropolar flow of liquid due to a perforated extending/shrinking interface containing quaternary nanoparticles and came to the conclusion that both the extending and pace of mass exchange have a significant impact on the overall structure of what is produced. Analysis of the effects of magnetohydrodynamic transfer of energy and mass over Casson fluid motion through a wedge with heat radiation and chemical processes was carried out by C. Sulochana *et al.* [6], who discovered that motion descriptions develop along heat and energy Grashof coefficients. In addition, the articles [7-10] mention some further noteworthy research on the transmission of heat and mass with a range of observable features. The heat source's role during fluid transportation is to enhance the fluid's thermal efficiency and raise the fluid's temperature. The aforementioned sources provide thermal energy, which may be applied to various tasks, including cooking, heating, and producing electricity. A study by M. A. Alghaseb *et al.* [11] used 3D numerical analysis to look into a room with good air flow and a single heat source. They found that where the heating device is placed has a big effect on how the flow behaves and how high it goes in the room when it is placed on a vertical surface close to the extraction opening. Jha and Samaila [12] establish the importance of the thermal source/sink on magnetohydrodynamics through free convection circulation in an upward channel through an applied field of magnetism. P. G. Metria *et al.* [13] have studied the MHD combined thermal boundary layer for viscoelastic fluid's movement across a stretched sheet immersed in an opaque medium in the midst of fluid dissipation and inconsistent sources of heat. Given its significant importance in space technology and the high distribution of temperatures, thermal radiation's effect on fluid flow can't be ignored. In this context, A.S. Idowu and U. Sani [14] revealed that an upsurge in the thermal exposure factor raises the fluid's temperature, which in turn lowers the fluid's viscosity, but a prominence in the domino effect attribute lowers the fluid's concentration. M. Prameela *et al.* [15] inquire into the detrimental effect of induction heat across MHD conveyance of fluid around a sphere. They use the fourth-order Runge-Kutta-Fehlberg strategy and MATHEMATICA programming to obtain computational solutions to differential equations, revealing that velocity profiles decrease with increasing magnetic field and thermal radiation parameters. By increasing the threshold of the radiation attribute, M. A. Kumar *et al.* [16] found that the temperature and velocity distributions of the inherent radiative nanofluid flow across an arbitrarily initiated vertical plate significantly improved. The authors, A. R. Hassan and O. J. Fenuga [17], look at how thermal radiation changes the path of a recurrent hydromagnetic tandem stress flow that moves along a navigable duct and is pushed by a heat source. Beyond that, certain well-known models have been built in response to noteworthy developments in thermal radiation [18-21]. The thermal dissemination impact, also known as the Soret (thermo-diffusion) effect, can't be

ignored when an object's mass moves radiatively because of a difference in temperature, as Eckert and Drake [20] say. This is because it can be used in engineering and research. G.V.R. Reddy and Y.H. Krishna [22] explored soret effects on the flow of a fluid with micropolar properties across a stretched sheet and into a porous, non-darcy petite and discovered that when the parameter of the soret effect increases, the flow rate of the boundary layer dimensions drops. A. K. Gautam *et al.* [23] investigate the combined convection layer of boundaries (MHD) movement of non-Newtonian Carreau fluid that encounters the effects of Soret and Dufour across an oscillating ascending plate. A. Quader and Md. M. Alam studied the transfer of unstable MHD convective mass and energy across a semi-infinite upward permeable sheet in an oscillating structure with the Soret effect, the Hall current, and constant heat flux [24]. The Soret effect on chemically emitted mhd oscillatory movement with a heat source through a perforated medium in an asymmetric curved stream has been studied by J. Sasikumar and A. Govindarajan [25]. They came to the conclusion from their research that oscillations in concentration profiles are caused by the combined effects of increasing the Soret number and a heat source parameter, whereas falls in concentration profiles are caused by an increase in the heat source parameter. Using an escalated upright plate and an opaque substance, M. A. Kumar *et al.* [26] assessed the repercussion Soret, Dufour, hall-current, and pivoting MHD instinctual convective transfer of energy and mass flow. When Schmidt and Dufour numbers, a chemical reaction parameter, rose to a certain point, they noticed that the concentration profile decreased and that, in comparison to the Soret numbers, a reversal pattern was seen. Nevertheless, it is well recognized that changes in temperature [27-29] may have a significant impact on a fluid's fundamental characteristics, making it challenging to forecast when a condition is safe or hazardous. This study unbiasedly investigates the significance of thermal radiation moving consistently along a porous medium with the intent to anticipate the flow behavior of the consequences of thermal radiation. The authors carefully went through an abundance of literature and found several studies on the effects of induction heat and thermal radiation on the MHD flow transfer of mass and radiation in the creation of numerous flow traits. Consequently, to their knowledge, no research has been accomplished using the effects of thermophoresis, chemical changes, and the heat source combined with aggregated transmission of heat and mass impact on the MHD fluid's flow. Thermophoresis and the heat source are incorporated along with other substantial flow properties, thereby facilitating the problem's uniqueness. By utilizing boundary-level estimates and indistinguishable transformations, the suggested model is made more efficient. The foundational coupled nonlinear group of equations is subsequently resolved using the numerical code of bvp4c in MATLAB.

2. Mathematical formulation

The Soret effect, thermal radiation, chemical reaction, and a heat source have all been taken into account in a 2-dimensional uniform free convective MHD flow that includes mass and heat transport over a heated upright permeable plate submerged in a porous medium. The $\bar{x}$-axis has been imagined as continuing vertically up the plate, and the $\bar{y}$-axis is perceived as parallel to it. Let $\bar{u}$ and $\bar{v}$ represent the fluid's relative $\bar{x}$ and $\bar{y}$-directional velocities. On the plate, a transverse magnetic field of strength B_0 is employed normally. Small Reynolds number causes the induced magnetic field to be ignored. For suction $v_0 < 0$. Since the motion is two-dimensional, x is independent of all physical variables.

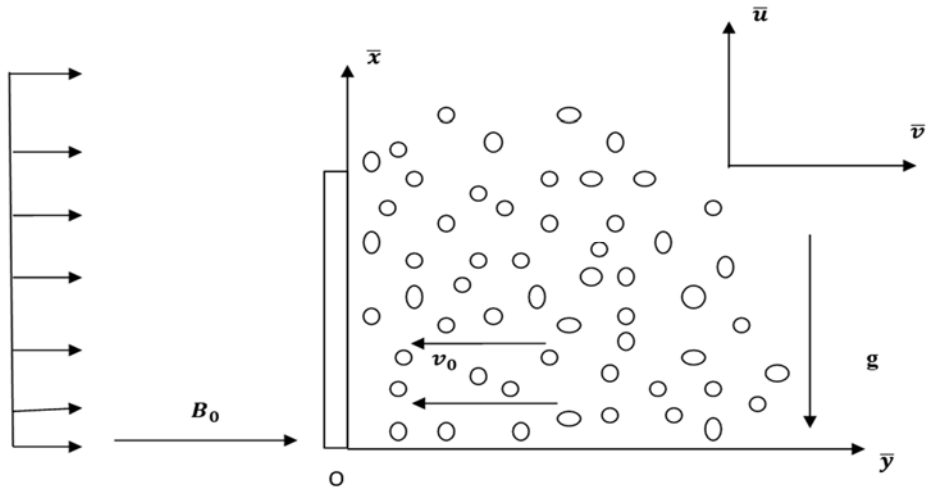

Fig.1. Physical model of the flow scheme.

Using the boundary surface appraisal [10], the governing equations are laid out in the subsequent chronology.

$$\frac{\partial \bar{v}}{\partial \bar{y}} = 0,$$

which implies

$$\bar{v} = -v_0 (v_0 > 0), \tag{2.1}$$

$$\bar{v}\frac{\partial \bar{u}}{\partial \bar{y}} = \nu \frac{\partial^2 \bar{u}}{\partial \bar{y}^2} + g\beta\left(\bar{T} - T_\infty\right) + g\beta^*\left(\bar{C} - C_\infty\right) - \frac{\sigma B_0^2 \bar{u}}{\rho} - \frac{\nu \bar{u}}{K_1}, \tag{2.2}$$

$$\bar{v}\frac{\partial \bar{T}}{\partial \bar{y}} = \frac{\kappa}{\rho C_P}\frac{\partial^2 \bar{T}}{\partial \bar{y}^2} - \frac{1}{\rho C_P}\frac{\partial \bar{q}_r}{\partial \bar{y}} + \frac{Q_h}{\rho C_P}\left(\bar{T} - T_\infty\right), \tag{2.3}$$

$$\bar{v}\frac{\partial \bar{C}}{\partial \bar{y}} = D_1 \frac{\partial^2 \bar{C}}{\partial \bar{y}^2} - K_C\left(\bar{C} - C_\infty\right) + \frac{D_m K_T}{T_m}\frac{\partial^2 \bar{T}}{\partial \bar{y}^2} \tag{2.4}$$

where $\bar{u}$ and $\bar{v}$ are velocity component along and perpendicular to the plane respectively, g is gravitational acceleration, B_0 is magnetic field strength, β is dimensional growth for transmitting heat, β^* is the transmission of mass aided by volumetric expansion, σ is electric conductivity, $\bar{T}$ is temperature of the fluid close to the plate, T_∞ is far-field temperature, $\bar{C}$ is fluid accumulation close to the plate, C_∞ is distant field concentration, ρ is fluid density, ν is kinematic viscosity, K_1 is permeability of porous medium, κ is thermal efficiency, C_P is the specific heat at persistent pressure, $\bar{q}_r$ is area-per-unit-heat flux, Q_h is heat generation coefficient, D_1 is molecular diffusivity, D_m is mass diffusion coefficient, K_C. is chemical reaction coefficient, K_T is thermal diffusion ration, T_m . is fluid mean temperature.

Using Rosseland approximation we get,

$$\overline{q}_r = -\frac{4\sigma_s}{3k_c}\frac{\partial \overline{T}^4}{\partial \overline{y}} \tag{2.5}$$

where k_c stands for the mean coefficient of absorbance and σ_s represents the Stefan Boltzmann parameter. Expanding $\overline{T}^4$ after excluding higher order terms, the Taylor Series about T_∞ has the form

$$\overline{T}^4 \cong 4T_\infty^3\overline{T} - 3T_\infty^4 .$$

Suitable boundary circumstances are:

$$\begin{aligned} &y = 0 : \overline{u} = 0, \quad \overline{T} = T_W, \quad \overline{C} = C_W, \\ &y \to \infty : \overline{u} \to 0, \quad \overline{T} \to T_\infty, \quad \overline{C} \to C_\infty . \end{aligned} \tag{2.6}$$

Dimensionless parameters are:

$$y = \frac{v_0\overline{y}}{\nu}, \quad u = \frac{\overline{u}}{v_0}, \quad \Pr = \frac{\mu C_P}{\kappa}, \quad \theta = \frac{\overline{T} - T_\infty}{T_W - T_\infty}, \quad \phi = \frac{\overline{C} - C_\infty}{C_W - C_\infty},$$

$$Gr = \frac{\nu g\beta(T_W - T_\infty)}{v_0^3}, \quad Gm = \frac{\nu g\beta^*(C_W - C_\infty)}{v_0^3}, \quad M = \frac{\sigma B_0^2\nu}{\rho v_0^2}, \quad Sc = \frac{\nu}{D_1}, \tag{2.7}$$

$$K = \frac{K_1 v_0^2}{\nu^2}, \quad Kr = \frac{\nu K_C}{v_0^2}, \quad R = \frac{\kappa k_C}{4\sigma_s T_\infty^3}, \quad Q = \frac{Q_h\nu}{\rho C_P v_0^2}, \quad So = \frac{D_m K_T (T_W - T_\infty)}{T_m (C_W - C_\infty)}.$$

Here y is dimensionless coordinate, μ is dynamic viscosity, Pr is Prandtl number, θ is non-dimensional temperature, ϕ is dimensionless concentration, Gr is the Grashof thermal number, Gm is an unambiguous Grashof number, M is magnetic aspect, Sc is Schmidt parameter, Kr is Chemical reaction coefficient, R is radiation factor, Q is heating source parameter, K is permeability of porous medium, So is Soret number Modified equations are

$$\frac{d^2u}{dy^2} + \frac{du}{dy} + Gr\theta + Gm\phi - Mu - \frac{u}{K} = 0 , \tag{2.8}$$

$$\frac{1}{\Pr}\left(1 + \frac{4}{3R}\right)\frac{d^2\theta}{dy^2} + \frac{d\theta}{dy} + Q\theta = 0 , \tag{2.9}$$

$$\frac{1}{Sc}\frac{d^2\phi}{dy^2} + \frac{d\phi}{dy} + So\frac{d^2\theta}{dy^2} - Kr\phi = 0 . \tag{2.10}$$

Enhanced modified circumstances at the boundaries:

$$\begin{aligned} &y = 0 : u = 0, \quad \theta = 1, \quad \phi = 1 \\ &y \to \infty : u \to 0, \quad \theta \to 0, \quad \phi \to 0 \end{aligned} \tag{2.11}$$

3. Validation of Code

Table 1 provides support for the correctness of the approach taken in this investigation. The comparison of shearing stress (σ) for permeability parameter (K) has been done with Raju *et al.* [30] setting $K = 1$.

Table 1. The correctness of the approach.

K	Raju *et al.*[28]	Present study
0.1	*1.8545*	*2.3131*
0.7	*3.2627*	*3.2913*
1	*3.2627*	*3.3767*

4. Method of solution

Due of the restrictions (2.11) along with initial conditions, the MATLAB bvp4c quantitative method is used for solving Eqs (2.8) to (2.10). One of the newest expansions to MATLAB, the bvp4c problem-solver yields superior results. MATLAB BVP solver, a finite difference algorithm that performs the three phases of the Lobatto IIIa formula, is used to find numerical outcomes. Shampine *et al.* [31-32] provide insight regarding the bvp4c technique. Here Eqs (2.8) to (2.10) are converted into a system of first-order equations utilizing MATLAB's built-in solver, bvp4c, as follows.
Let

$$u = y(1), \quad \frac{du}{dy} = y(2), \quad \theta = y(3), \quad \frac{d\theta}{dy} = y(4), \quad \phi = y(5), \quad \frac{d\phi}{dy} = y(6),$$

which gives

$$\begin{aligned} dydx = \big[& y(2) - y(2) - Gr * y(3) - Gm * y(5) + \\ & + M * y(1) + (1/K) * y(1) y(4) \big(-y(4) - Q * y(3)\big) * \big(Pr / (1 + 4/3 * R)\big) y(6) + \\ & - y(6) * Sc - So * \big(-y(4) - Q * y(3)\big) * \big(Pr / (1 + 4/3 * R)\big) * Sc + Kr * y(5) * Sc \big]. \end{aligned}$$

5. Results and discussions

In order to assess the problem's physical significance, quantitative estimates of velocity, temperature, and concentration were all made using a variety of estimates of suitable dimensionless flow characteristics. Begin by gathering a set of arbitrary attributes with values, among which are $Gr = 1$, $Gm = 2$, $K = 0.25$, $M = 2$, $Pr = 1$, $Sc = 0.1$, $Kr = 1$, $So = 0.5$, $R = 0.2$, and $Q = 0.5$, unless otherwise stated. The velocity curves incorporated into various fluid characteristics are shown in Figs 2-7. The velocity profile for various effects of M is shown in Fig.2. The illustration demonstrates that elevating the magnetic value M inhibits the flow rate. Because of the strong magnetism occurring during the fluid's normal flow and causing resistance within the particles, the fluid's velocity drops. So, enormous resistance or friction acts like a drag or a kind of

"magnetic rigidity" for a transmissible fluid, which prevents fluid flow. Inevitably, it switches away particles of fluid that are susceptible to additional limitations that often hinder their voyage across the fluid's channel. The fluid's overall rate of flow becomes antagonistic as a consequence of this loss of velocity.
The Prandtl number demonstrates the synergy between thermal diffusivity and fluid motion characteristics. Figure 3 serves as an illustration of how energy travels through the fluid more effectively than momentum does. Figure 4 illustrates the velocity curve's changed appearance as So has grown. As the thermophoretic parameter increases, the Soret effect's adverse consequences become more pronounced. In real terms, the twirling of the floating aspects in response to their thermal disparity may have an effect on the total flow rate and alter the distribution of velocity. The velocity spectrum may be altered as a result of this effect, leading to increased velocities in specific fluid areas. When attempting to comprehend how alteration in reaction characteristics impacts flow rate, it is crucial to take into account the chemical reaction attribute and its related enthalpy aspects. The fluid's viscosity might rise as a result of chemical processes. Figure 5 depicts how fluid velocity decreases as viscosity grows, which renders the fluid more challenging to flow through.

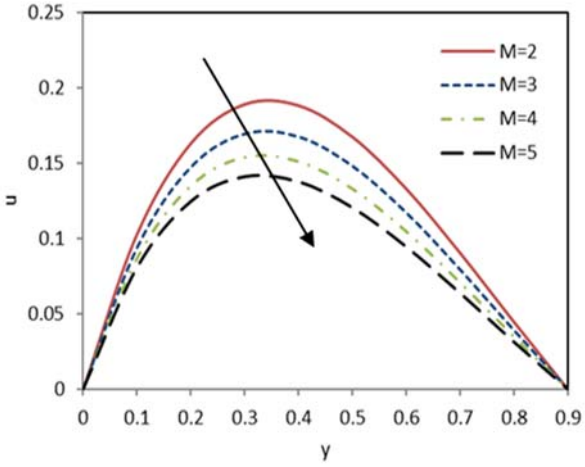

Fig.2. Velocity outline for varying M .

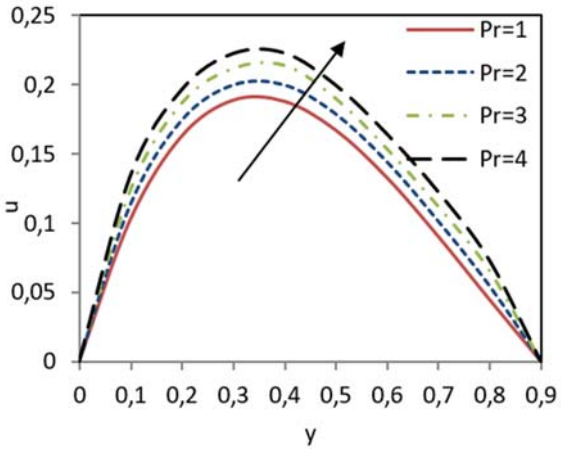

Fig.3. Velocity outline for varying Pr .

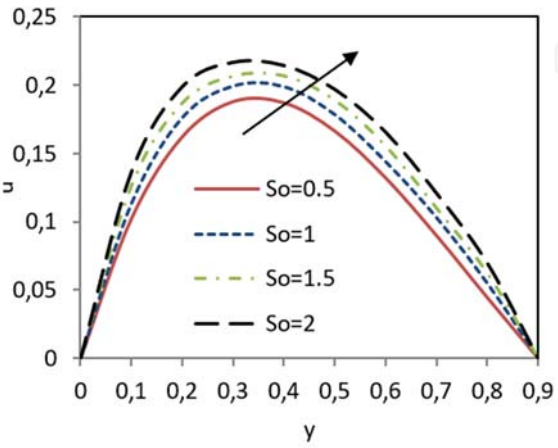

Fig.4. Velocity outline for varying So .

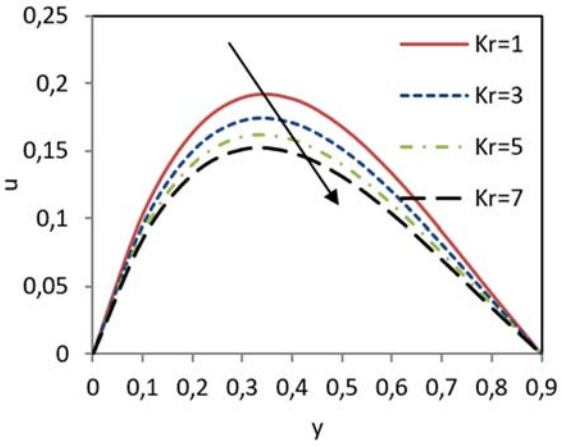

Fig.5. Velocity outline for varying Kr .

The more prominent aspect of the velocity portrayal, however, is shown in Fig.6 when Gr is raised. As the Grashof value rises, buoyant forces begin to dominate instead of viscous pressure, which had previously controlled the fluid's motion. The speed of presentation dramatically increases as it comes to a close. As the

permeability factor K varies, velocity trends are shown in Fig.7. From the aforementioned picture, it can be seen that when the porousness index K increases, the flow rate of the fluid rises. The rate of flow of the fluid across a medium that is porous physically increases with a rise in porosity. The medium's impedance may be brushed aside as the permeable medium's pores grow in size. Accordingly, the velocity is shown to be zero at the beginning and gradually increases as it approaches the free surface, where it achieves its maximum. Figure 8 describes velocity for various values of thermal radiation R. It is notices that with the growth of R, velocity boost up.

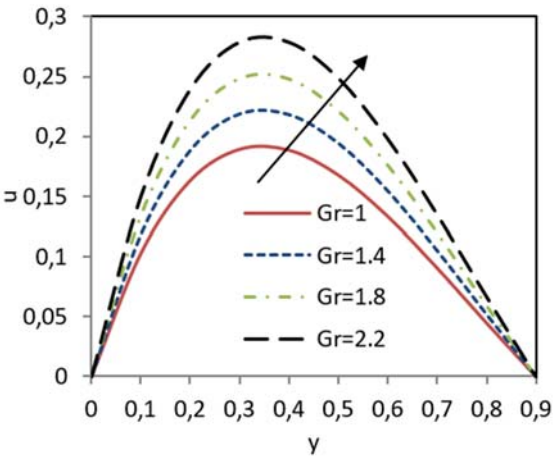

Fig.6. Velocity outline for varying Gr.

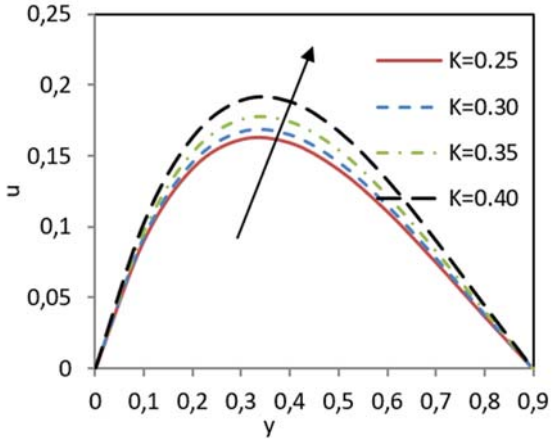

Fig.7. Velocity outline for varying K.

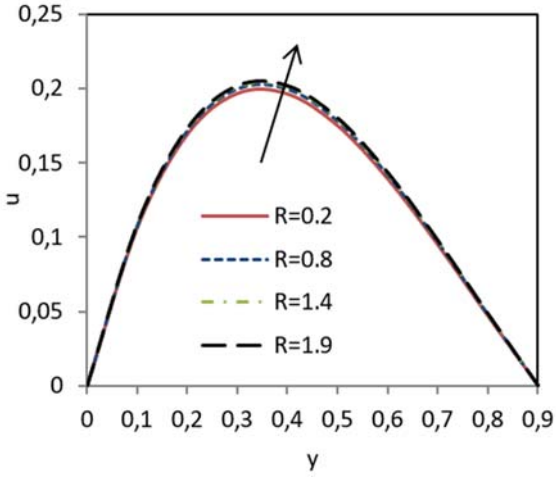

Fig.8. Velocity outline for varying R.

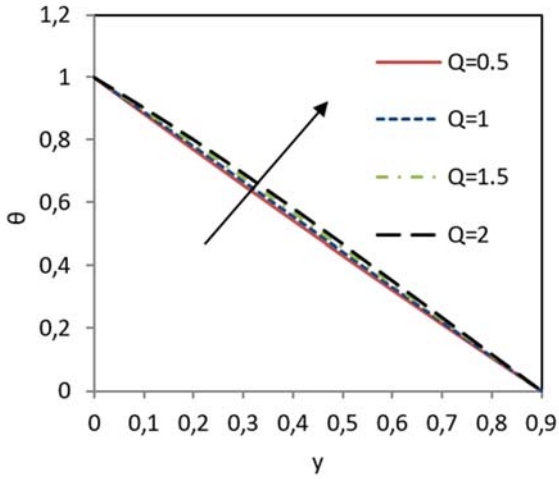

Fig.9. Temperature outline for varying Q.

Figures 9-11 show several temperature prospects suitable for various fluid properties. The input of thermal energy to the entire system causes the internal temperature to rise normally when the heat source factor Q is increased, as shown in Fig.9. The correlation between the viscosity of a fluid throughout the transition and its thermal dissemination efficiency is described by the Prandtl number, which is an unconstrained number. It indicates the size of the disparity between momentum expansion and heat expansion during the motion of a fluid. A higher Prandtl value shows that momentum expansion is less significant as compared to thermal diffusion. If the Prandtl number is bigger, there might be less of a temperature difference when fluids are

moving, especially through the interface layer of an opaque surface, as shown in Fig.10. This is because heat moves more quickly than momentum. R increases the significance of heat transmission through radiation.

The conveyance of heat by ionizing radiation waves is a component of the influence of radiation transfer. The temperature differential might decline as radiation becomes more pervasive in all facets of the heat exchange process, as shown in Fig.11. Different concentration distributions are shown in Figs 12-16. A more substantial heat source component causes additional temperature variations or shifts in temperature in systems involving the transport of mass and heat exchange. Propagation of the concentration differences may proceed more quickly as a result. If the concentration is moving as a consequence of diffusion, a faster rate of diffusion might cause a quicker drop in concentration, which will reduce the concentration gradient, as clearly shown in Fig.12.

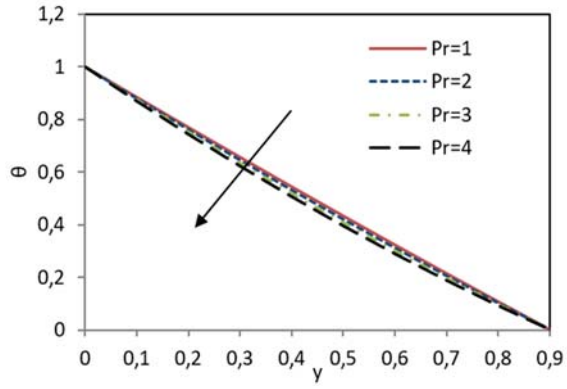

Fig.10. Temperature outline for varying Pr.

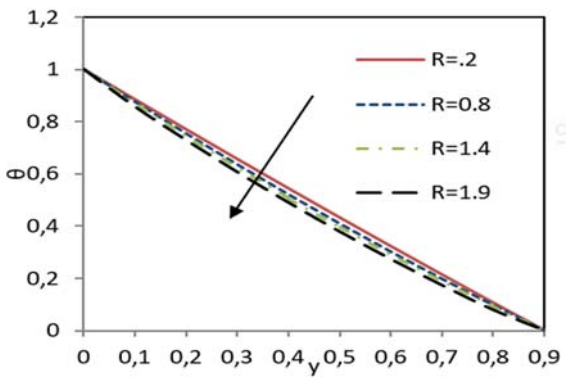

Fig.11. Temperature outline for varying R.

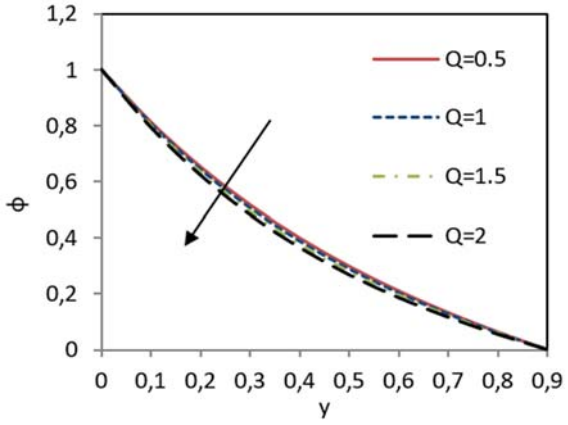

Fig.12. Concentration outline for varying Q.

Due to Soret effect or thermophoresis, particles or solute molecules can concentrate or dwindle in particular areas of the thermal disparity. The solute will build up in the more radiant parts, increasing their concentration persona, as seen in Fig.13 if the Soret index is positive (showing that particles travel from cooler to hotter locations). When the chemical reaction parameter is raised, Fig.14 shows a diminutive change in the concentration gradient. Because of the increasing Prandtl number, Fig.15 shows that concentration variations are increasingly prominent. Figure 16 shows increasing profile of concentration with the rise of R.

According to various flow properties, Tables 2, 3, and 4 highlight various values of shearing stress, Nusselt number, and Sherwood number. Table 2 demonstrates that shearing stress increases with increasing Grashof and Prandtl numbers but reduces with increasing magnetic field number, chemical reaction factor, and porosity parameter. Table 3 demonstrates how the Prandtl and radiation characteristics increase the Nusselt

value while the thermal source variable reduces it. The Sherwood number rises with the chemical responses factor and falls with the Soret consequence, as seen in Table 4.

Table 2. Shearing stress (σ).

M	Gr	Gm	Pr	K	Sc	R	Q	So	Kr	Shearing stress (σ)	
2	1	2	1	0.25	0.1	0.2	0.5	1	1	1.1420	↓
3										1.0550	
4										0.9844	
5										0.9258	
2	1	2	1	0.25	0.1	0.2	0.5	1	1	1.1420	↑
	1.4									1.3140	
	1.8									1.4861	
	2.2									1.5722	
2	1	2	1	0.25	0.1	0.2	0.5	1	1	1.1420	↑
			2							1.1472	
			3							1.1524	
			4							1.1577	
2	1	2	1	0.25	0.1	0.2	0.5	1	1	1.1420	↓
				0.30						1.0819	
				0.35						1.0440	
				0.40						1.0180	
2	1	2	1	0.25	0.1	0.2	0.5	1	1	1.1648	↓
									3	1.1420	
									5	1.1210	
									7	1.1017	

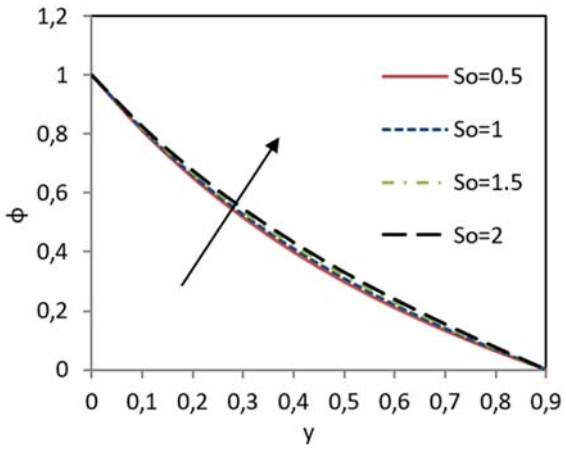

Fig.13. Concentration outline for varying So.

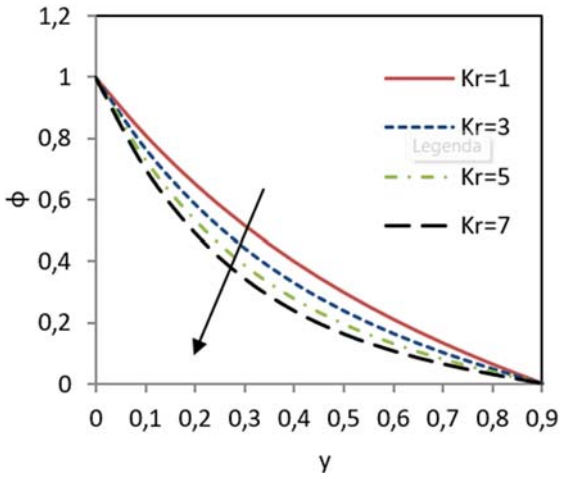

Fig.14. Concentration outline for varying Kr.

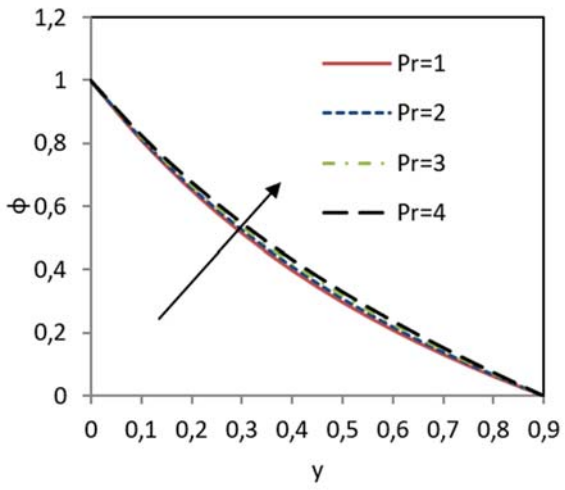

Fig.15. Concentration outline for varying Pr .

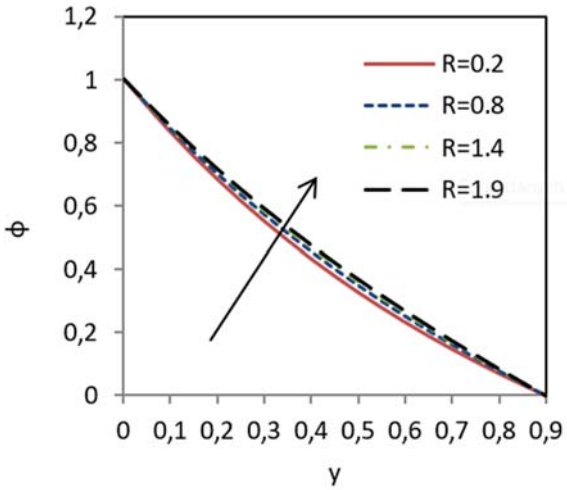

Fig.16. Concentration outline for varying R .

Table 3. Nusselt's Number

Pr	*M*	*Gr*	*Gm*	*Q*	*K*	*Kr*	*R*	*So*	*Sc*	Nusselt's No. (Nu)	
1	*2*	*1*	*2*	*0.5*	*0.25*	*1*	*0.2*	*1`*	*0.1*	*1.0448*	↑
2										*1.0923*	
3										*1.1426*	
4										*1.1958*	
1	*2*	*1*	*2*	*0.5*	*0.25*	*1*	*0.2*	*1*	*0.1*	*1.0448*	↓
				1						*1.0228*	
				1.5						*1.0006*	
				2						*0.9782*	
1	*2*	*1*	*2*	*0.5*	*0.25*	*1*	*0.2*			*1.0448*	↑
							0.8			*1.1362*	
							1.4			*1.1918*	
							1.9			*1.2237*	

Table 4. Sherwood Number.

Pr	*M*	*Gr*	*Gm*	*Q*	*K*	*Kr*	*R*	*So*	*Sc*	Sherwood No. (Sh)	
1	*2*	*1*	*2*	*0.5*	*0.25*	*1*	*0.2*	*1`*	*0.1*	*1.6877*	↑
						3				*1.8371*	
						7				*1.9784*	
						9				*2.1124*	
1	*2*	*1*	*2*	*0.5*	*0.25*	*1*	*0.2*	*0.5*	*0.1*	*1.8614*	↓
								1		*1.8371*	
								1.5		*1.8129*	
								2		*1.7887*	

6. Conclusions

The implications of concentration, as well as temperature changes, thermal analysis in conjunction with thermal and chemical reactions, and the consequential impact of a relevant external electromagnetic spectrum on the transfer of mass and energy within a heat-generating fluid via permeable media, are modelled as coupled non-linear circumstances with an ideal boundary zone. In light of the foregoing query, the following major points are revealed:

- The motion, temperature, and concentration subdomains in the fluid area's oscillating movements simulate radiation. This is due to the pulsating oscillations of the flow characteristics.
- It can be seen that the velocity improves significantly in each of the representations before beginning to decline.
- The Soret phenomenon and the influence of the electromagnetic field slow down fluid velocity. With the rise of magnetic parameter, there exists a resistance force called Lorentz force between the fluid layers which causes velocity drops.
- However, it is accelerated by the Soret effect, while it speeds up with the Prandtl number, radiation parameter and the thermal Grashof number, it slows down with the chemical response parameter estimation.
- Although the source of heat component speeds it up, the radiation factor and Prandtl number both slow down the fluid's temperature.
- The Prandtl number, radiation and the thermophoretic effect both lead to a rise in fluid concentration, but the parameters governing the chemical reaction and the heat source have the opposite impact.
- Under the restrictions of the various fluid specifications, the strength of the drag force against a particular flow parameter leaves a discernible impact. Additionally, a noteworthy influence on the Nusselt number and Sherwood number is exerted by the specific fluid characteristics.

Future Scope:

Other numerical techniques have also been successful in resolving this issue. The approach to this issue can be extended to other intricate geometrical configurations. This problem could be expanded to include a variety of non-Newtonian models. It is possible to implement various significant physical properties and watch how they affect the flow fluid. Thus, there is a wealth of untapped research potential.

Nomenclature

B_0 – magnetic field strength

$\overline{C}$ – fluid accumulation close to the plate

C_∞ – distant field concentration,

C_P – the specific heat at persistent pressure

D_l – molecular diffusivity

D_m – mass diffusion coefficient

g – gravitational acceleration

K_C – chemical reaction coefficient

K_T – thermal diffusion ration

Gr – the Grashof thermal number,

Gm – an unambiguous Grashof number

K – permeability of porous medium

Kr – chemical reaction coefficient

K_1 – permeability of porous medium

k_c – stands for the mean coefficient of absorbance,

M – magnetic aspect

Pr – Prandtl number

Q – heat source parameter

Q_h – heat generation coefficient

$\bar{q}_r$ – area-per-unit-heat flux

R – radiation factor,

Sc – Schmidt parameter

So – Soret number

$\bar{T}$ – temperature of the fluid close to the plate,

T_m – fluid mean temperature.

T_∞ – far-field temperature,

$\bar{u}$ and $\bar{v}$ – velocity component along and perpendicular to the plane respectively

y – dimensionless coordinate,

β – dimensional growth for transmitting heat

β^* – the transmission of mass aided by volumetric expansion

θ – non-dimensional temperature,

κ – thermal efficiency

μ – dynamic viscosity

ν – kinematic viscosity

ρ – fluid density,

σ – electric conductivity,

σ_s – the Stefan Boltzmann parameter

ϕ – dimensionless concentration

References:

[1] Ene R. D., Pop N. and Badarau R. (2023): *Heat and mass transfer analysis for the viscous fluid flow dual approximate solutions*.– Mathematics., vol.11, No.7, pp.1-22.

[2] Qureshi I. H., Nawaz M., Abdel-Sattar M. A., Aly S. and Awais M. (2021): *Numerical study of heat and mass transfer in MHD flow of nanofluid in a porous medium with Soret and Dufour effects*.– Heat Transfer., vol.50, No.5, pp.4501-4515.

[3] Fatunmbi E. O. and Adeniyan A. (2018): *Heat and mass transfer in MHD micropolar fluid flow over a stretching sheet with velocity and thermal slip conditions*.– Open Journal of Fluid Dynamics., vol.8, pp.195-215.

[4] Agaie B. G., Isa S., Mai'anguwa A. S. A., and Magaji A. S. (2021). *Heat and mass transfer of MHD for an unsteady viscous oscillatory flow*.– Science World Journal., vol.16, No.2, pp.138-144.

[5] Vanitha G.P., Mahabaleshwar U.S., Hatami M. and Yang X. (2023): *Heat and mass transfer of micropolar liquid flow due to porous stretching/shrinking surface with ternary nanoparticles*.– Scientific Reports., vol.13, No.1, pp.1-17.

[6] Sulochana C., Aparna S. R. and Sandeep N. (2021): *Heat and mass transfer of magnetohydrodynamic Casson fluid flow over a wedge with thermal radiation and chemical reaction*.– Heat transfer., vol.50, No.4, pp.3704-3721.

[7] Dey B., Nath J. M., Das T. K. and Kalita D. (2022): *Simulation of transmission of heat on viscous fluid flow with varying temperatures over a flat plate*.– JP Journal of Heat and Mass Transfer., vol.30, pp.1-18.
[8] Dey B. and Choudhury R. (2019): Slip effects on heat and mass transfer in MHD visco-elastic fluid flow through a porous channel.– *In Emerging Technologies in Data Mining and Information Security*.– Proceedings of IEMIS, Springer Singapore., vol.1, pp.553-564.
[9] Choudhury R., Dey B. and Das B. (2018): *Hydromagnetic oscillatory slip flow of a visco-elastic fluid through a porous channel*.– Chemical Engineering Transactions., vol.71, pp.961-966.
[10] Choudhury R. and Kumar Das S. (2014): *Visco-elastic MHD free convective flow through porous media in presence of radiation and chemical reaction with heat and mass transfer*.– Journal of Applied Fluid Mechanics., vol.7, No.4, pp.603-609.
[11] Alghaseb M. A., Hassen W., Mesloub A., and Kolsi L. (2022): *Effect of heat source position in fluid flow, heat transfer and entropy generation in a naturally ventilated room*.– Mathematics., vol.10, No.2, pp.1-23.
[12] Jha B. K. and Samaila G. (2020): *Effect of heat source/sink on MHD free convection flow in a channel filled with nanofluid in the existence of induced magnetic field: an analytic approach*.– SN Applied Sciences., vol.2, pp.1-15.
[13] Metri P. G., Metri P. G., Abel S. and Silvestrov S. (2016): *Heat transfer in MHD mixed convection viscoelastic fluid flow over a stretching sheet embedded in a porous medium with viscous dissipation and non-uniform heatsource/sink*.– Procedia Engineering., vol.157, pp.309-316.
[14] Idowu A. S. and Sani U. (2019): *Thermal radiation and chemical reaction effects on unsteady magnetohydrodynamic third grade fluid flow between stationary and oscillating plates*.– International Journal of Applied Mechanics and Engineering., vol.24, No.2, pp.269-293.
[15] Prameela M., Lakshmi D. V. and Gurejala J. R. (2021): *Influence of thermal radiation on MHD fluid flow over a sphere*.– Biointerface Research in Applied Chemistry., vol.12, No.5, pp.6978-6990
[16] Kumar M. A., ReddyY. D., Rao V. S. and Goud B. S. (2021): *Thermal radiation impact on MHD heat transfernatural convective nanofluid flow over an impulsively started vertical plate*.– Case Studies in Thermal Engineering, vol.24, pp.1-10.
[17] Hassan A. R. and Fenuga O. J. (2019): *The effects of thermal radiation on the flow of a reactive hydromagneticheat generating couple stress fluid through a porous channel*.– SN Applied Sciences., vol.1, pp.1-10.
[18] Dey B., Kalita, B. and Choudhury R. (2022): *Radiation and chemical reaction effects on unsteady viscoelastic fluid flow through porous medium*.– Frontiers in Heat and Mass Transfer (FHMT)., vol.18, pp.1-8.
[19] Haldar S., Mukhopadhyay S. and Layek G. C. (2021): *Effects of thermal radiation on Eyring–Powell fluid flow and heat transfer over a power-law stretching permeable surface*.– International Journal for Computational Methods in Engineering Science and Mechanics., vol.22, No.5, pp.366-375.
[20] Sahoo A. and Nandkeolyar R. (2021): *Entropy generation and dissipative heat transfer analysis of mixed convective hydromagnetic flow of a Casson nanofluid with thermal radiation and Hall current*.– Scientific Reports., vol.11, No.1, pp.1-31.
[21] Eckert E. R. and Drake Jr R. M. (1987): *Analysis of heat and mass transfer*.– Hemisphere Publishing; New York., vol.19, No.23, pp.1-806.
[22] Reddy G. V. R. and Krishna Y. H. (2018): *Soret and Dufour effects on MHD micropolar fluid flow over a linearly stretching sheet, through a non-Darcy porous medium*.– International Journal of Applied Mechanics and Engineering., vol.23, No.2, pp.485-502.
[23] Gautam A. K., Verma A. K., Bhattacharyya K. and Banerjee A. (2020): *Soret and Dufour effects on MHD boundary layer flow of non-Newtonian Carreau fluid with mixed convective heat and mass transfer over a moving vertical plate*.– Pramana, vol.94, pp.1-10.
[24] Quader A. and Alam M. M. (2021): S*oret and dufour effects on unsteady free convection fluid flow in the presence of Hall current and heat flux*.– Journal of Applied Mathematics and Physics., vol.9, pp.1611-1638.
[25] Sasikumar J. and Govindarajan A. (2018): *Soret effect on chemically radiating MHD oscillatory flow with heat source through porous medium in asymmetric wavy channel*.– In Journal of Physics: Conference SeriesIOP Publishing., vol.1000, No.1, pp.1-12.
[26] Kumar M. A., Reddy Y. D., Goud B. S. and Rao V. S. (2021): *Effects of Soret, Dufour, Hall current, and rotation on MHD natural convective heat and mass transfer flow past an accelerated vertical plate through a porous medium*.– International Journal of Thermofluids., vol.9, pp.1-9.
[27] Kabir M. A. and Al Mahbub M. A. (2012): *Effects of thermophoresis on unsteady MHD free convective heat and mass transfer along an inclined porous plate with heat generation in presence of magnetic field*.– Open Journal of Fluid Dynamics, vol.2 No.4, Article ID:25497, p.4, DOI:10.4236/ojfd.2012.24012

[28] Sheikholeslami M., Ganji D. D., Javed M. Y., and Ellahi R. (2015): *Effect of thermal radiation on magnetohydrodynamics nanofluid flow and heat transfer by means of two-phase model*.– Journal of Magnetism and Magnetic Materials, vol.374, pp.36-43.
[29] Das K. (2012): *Influence of thermophoresis and chemical reaction on MHD micropolar fluid flow with variable fluid properties*.– International journal of heat and mass transfer., vol.55, pp.7166-7174.
[30] Raju M. C., Verma S.V. K., and Anandareddy N. (2012): *Radiation and mass transfer effects on a free convective flow through a porous media bounded by vertical surface*.– Journal on Future Engineering & Technology, vol.7, No.2, pp.7-12.
[31] Shampine L. F., Gladwell I., and Thompson S. (2003): *Solving ODEs with Matlab*.– Cambridge University Press.
[32] Kierzenka J., and Shampine L. F. (2001): *A BVP solver based on residual control and the Maltab PSE*.– ACM Transactions on Mathematical Software (TOMS), vol.27, No.3, pp.299-316.

Received: October 16, 2023
Revised: January 17, 2024